World Journal of Pharmaceutical Science and Research
www.wjpsronline.com
Research Article
ISSN: 2583-6579
SJIF Impact Factor: 5.111
Year - 2024
Volume: 3; Issue: 5
Page: 454-478

IONIC NANOMEDICINE STRATEGY TO DEVELOP EFFECTIVE CHEMO-PTT COMBINATION CANCER THERAPEUTICS

Mujeebat Bashiru[1], Mavis Forson[1], Arisha Ishtiaq[1], Adeniyi Oyebade[1], Samantha Macchi[1], Shehzad Sayyed[2], Nawab Ali[3], Robert J. Griffin[4], Adegboyega K. Oyelere[5] and Noureen Siraj[1*]

[1]Department of Chemistry, University of Arkansas at Little Rock, Little Rock, AR 72204, USA.
[2]Department of Chemistry, University of Arkansas at Fayetteville, AR 72701, USA.
[3]Department of Biology, University of Arkansas at Little Rock, Little Rock, AR 72204, USA.
[4]University of Arkansas for Medical Sciences, Winthrop P. Rockefeller Cancer Institute, Arkansas Nanomedicine Center, Department of Radiation Oncology, 4301 W Markham St, Little Rock, AR 72205, USA.
[5]School of Chemistry and Biochemistry, Parker H. Petit Institute for Bioengineering and Bioscience, Georgia Institute of Technology, Atlanta, Georgia 30332, USA.

Article Received: 21 August 2024 | | ***Article Revised: 09 October 2024*** | | ***Article Accepted: 30 November 2024***

***Corresponding Author: Noureen Siraj**
Department of Chemistry, University of Arkansas at Little Rock, Little Rock, AR 72204, USA.
DOI: https://doi.org/10.5281/zenodo.14146024

How to cite this Article: Mujeebat Bashiru, Mavis Forson, Arisha Ishtiaq, Adeniyi Oyebade, Samantha Macchi, Shehzad Sayyed, Nawab Ali, Robert J. Griffin, Adegboyega K. Oyelere and Noureen Siraj (2024). IONIC NANOMEDICINE STRATEGY TO DEVELOP EFFECTIVE CHEMO-PTT COMBINATION CANCER THERAPEUTICS. World Journal of Pharmaceutical Science and Research, 3(5), 454-478. https://doi.org/10.5281/zenodo.14146024

ABSTRACT

Herein, a detailed investigation of nanodrugs derived by combining a chemotherapy (chemo) and photothermal therapy (PTT) approaches to enhance chemo drug efficacy is presented. Tamoxifen and its metabolite; N-desmethyltamoxifen are the selected chemo drugs that were electrostatically attached with a PTT agent, NaIR820, via a metathesis approach to develop two different ionic material (IM)-based chemo-PTT drugs. Ionic nanomaterials (INMs) were synthesized using reprecipitation method, and these carrier- free nanoparticles were characterized in detail. Photophysical properties of NaIR820 parent compound, and their derived chemo-PTT IMs and INMs revealed significant alterations in absorption and fluorescence emission spectra of IR820. Photophysical results demonstrated that INMs exhibited promising characteristics as photothermal agents that are beneficial for light mediated therapy. Photothermal conversion efficiency and reactive oxygen quantum yield of INMs and IMs also improved significantly in comparison to the parent NaIR820 compound. In vitro cell viability studies demonstrated improved dark and light cytotoxicity of chemo-PTT INMs as compared to treatments that involved either the mixture of both soluble parent drugs and chemo or PTT drugs independently. Moreso, apoptotic cell death signal was greatly enhanced for the INMs as opposed to the parent chemo drugs.

KEYWORDS: Tamoxifen, Ionic nanomedicine, Cytotoxicity, Combination index, Cell death mechanism.

1. INTRODUCTION

Tamoxifen (Nolvadex) is a FDA approved antiestrogen medication used as a prophylactic against breast cancer and also as an adjuvant to the primary disease.[1–3] It is also known to suppress P-gp (polyglycoprotein).[4,5] Tamoxifen (TAM) has also been examined for a variety of diseases, including infertility, gynecomastia, cardiovascular conditions, bipolar disorder, colon and rectal cancer.[4] The three active TAM's metabolites found in the human body by pharmacological test are N-desmethyltamoxifen (NDMTAM), 4-hydroxy-N-desmethyltamoxifen and 4-hydroxy-tamoxifen.[5] Of these three, NDMTAM is the major metabolite with closest bioactivity to TAM.[2,5] Although TAM is prescribed to women with estrogen receptor (ER)-α-positive breast cancer, but it causes adverse effects such as resistance and increased risk of endometrial cancer.[2,6–8] Therefore, researchers are exploring new strategies to increase TAM's effectiveness.

Malignant cells are recognized for displaying diverse characteristics such as unclear mechanisms responsible for cell proliferation, metabolism and defense which impact the resultant toxicity towards cancerous cells upon different treatments.[9,10] These properties makes it difficult for monotherapy to completely eradicate malignant lesions.[3] MCF-7 is a receptor positive breast cancer cell line that is highly responsive to TAM.[3] Literature reports reveal that TAM exhibits a high half maximal inhibitory concentration (IC_{50}) on MCF-7 cells and its cytotoxic response are typically observed at longer period of drug's incubation.[5,11] Therefore, any additional improvement in TAM's potency could positively impact the treatment outcomes for hormone-positive breast cancer patients.

Many approaches have been utilized to enhance the TAM's potency and lessen its side effects. These approaches include liposomal formulation[1], drug encapsulation via micelle formulation,[12] combination strategies,[13] and optimization with other medication types like metformin.[8,14] Among these, the use of combination strategies have been reported to effectively treat drug-resistant tumors.[12,15] An example of combination therapy is the incorporation of non-invasive light mediated therapy like photothermal therapy (PTT) along with chemotherapy (chemo). Thus, TAM's optimization in the presence of photothermal agents (PTAs) would introduce multiple mechanistic routes that will possibly target the cells differently and ultimately result in enhanced cytotoxic response.

Recently, our group showed that combination drug prepared by combining chemo (doxorubicin-'DOX') and PTT (NaIR820) exhibited enhanced synergy and improved toxicity in MCF-7 breast cancer cells.[16] The resultant combination drug, (DOX-PTT) exhibited Förster resonance energy transfer (FRET) capabilities that helped to improve the drug's PTT effect and allowed for investigation at either the donor's or the acceptor's excitation wavelength.[16] To enhance the cytotoxicity of TAM, a similar strategy was employed to obtain a TAM-PTT combination drug. However, a significant challenge is that the TAM-PTT combination drug lacks the FRET mechanism, which was present in DOX-PTT drug. This study is designed to answer whether FRET mechanism is essential to enhance the chemo-PTT INM's toxicity or only nanoparticle morphology is essential to attain lower IC_{50}.

Therefore, this work is designed to develop two chemo-PTT combination ionic materials (IMs) by combining TAM or NDMTAM and IR820, to produce [TAM][IR820] and [NDMTAM][IR820] with no FRET capabilities. In both [TAM][IR820] and [NDMTAM][IR820], there is no transfer of energy (FRET) from the donor to the acceptor since TAM or NDMTAM does not fluoresce. Thus, there is lack of spectra overlap between TAM or NDMTAM emission spectra and IR820 absorption spectra. These IMs were synthesized by implementing ionic liquid (IL) chemistry, simply by substituting the small counterion (chloride) present in TAM or NDMTAM with IR820 bulky anion. These two IMs

were converted into carrier-free ionic nanomaterials (INMs) via simple reprecipitation method in aqueous media and used to treat MCF-7 cancer cells. Thus, this project is aimed to determine whether the presence of FRET mechanism is essential or if nanoparticle's (INMs) morphology can impact the drug's efficacy. To completely understand the significance of IMs, we also devised a separate experiment involving the mixture of the two parent drugs (1:1 mixture of chemo and PTT) without counterions (Na^+ and Cl^-) removal. This allowed us to better appreciate the significance of IMs via IL chemistry to design combination drugs after eliminating spectator counterions.

2. EXPERIMENTAL

2.1 Chemicals

Tamoxifen (TAM), 2-[2-[2-chloro-3-[[1,3-dihydro-1,1-dimethyl-3-(4-sulfobutyl)-2H-benzo[e]indol-2-ylidene]-ethylidene]-1-cyclohexen-1-yl]-ethenyl]-1,1-dimethyl-3-(4-sulfobutyl)-1H-benzo[e]indolium hydroxide inner salt, sodium salt (NaIR820, Lot # SHBM1333), Phosphate buffer (PBS) pH 7.4, 1.3-diphenylisobenzofuran (DPBF, Lot # STBD0599V), concentrated hydrochloric acid (HCl) and dimethyl sulfoxide (DMSO) were purchased from Sigma-Aldrich, (ST. Louis, MO). Triply deionized water (18.2 MΩ cm) was obtained via a pure lab Ultrapure water purification system (ELGA, Woodridge, IL). Dichloromethane (DCM) and ethanol were of ACS grade and sourced from Thermo Fischer (Waltham, MA). 808 nm laser was purchased from Opto Engine LLC (Midvale, UT, US). MCF-7 cancerous cells were purchased from American Type Culture Collection (ATCC, Manassas, VA). Cell media (Dulbecco's Modified Eagles Medium (DMEM), MTT (3-(4,5-dimethylthiazol-2-yl)-2,5-diphenyltetrazolium bromide), fetal bovine serum (FBS) was obtained from Atlanta Biologicals (Lawrenceville, GA). Penicillin streptomycin, and Trypsin-EDTA (0.25%) were purchased from Caisson Lab (Smithfield, UT). Oxazole yellow oxide (YO-PRO 1) (LOT # 1597071) was purchased from Thermo Fisher Scientific and propidium iodide (PI) (Lot # 21P0211) was obtained from Biotium company (Fremont, CA).

2.2 Synthesis and characterization of tamoxifen-based chemo combination drugs

Synthesis of TAM-based chemo-combination drugs involve a facile, rapid, economical biphasic ion exchange method. TAM was first converted to its acidic salt (tamoxifen hydrochloride) by reacting with equivalent mole ratio of HCl in ether according to synthesis scheme in Figure 1 below. The salt form was isolated, and solid precipitate was recrystallized. TAM hydrochloride (TAM.HCl), the chemotherapeutic drug was dissolved in DCM, while NaIR820 was dissolved in water. For [TAM][IR820] synthesis, equivalent mole ratios of TAM.HCl i.e, (100mg) and NaIR820 (222.6mg) solution previously prepared in DCM and water separately were combined and stirred for 24 hr at room temperature for complete ion exchange reaction. Water layer containing sodium chloride (spectator counterions) was discarded, and the organic layer was washed repeatedly with water to get rid of any remaining salt. The aqueous layer was tested with silver nitrate to ensure complete removal of chloride ions in the reaction vessel. The organic layer containing the product was dried via rotary evaporator to remove the DCM, and the resultant [TAM][IR820] IM was subjected to lyophilization to eliminate the excess moisture prior to further studies.

Similarly, [NDMTAM]Cl was used to synthesize [NDMTAM][IR820] IM using the same protocol stated above. Synthesis scheme for [NDMTAM][IR820] IM was reported in Figure S1 of the supporting information (SI). All chemo-PTT combination IMs were characterized using electrospray ionization mass spectrometry (ESI-MS), which was performed using a Bruker (Billerica, MA) Ultraflex 9.4T in methanol solvent, and the results are shown in Figure S2. The combination drugs was confirmed using mass to charge ratio peaks. These chemo-PTT IMs are further

characterized using ^{1}H-NMR recorded on a JEOL 400 MHz nuclear magnetic resonance instrument, employing deuterated dimethyl sulfoxide (DMSO) as solvent system. NMR results are reported in Figure S3.

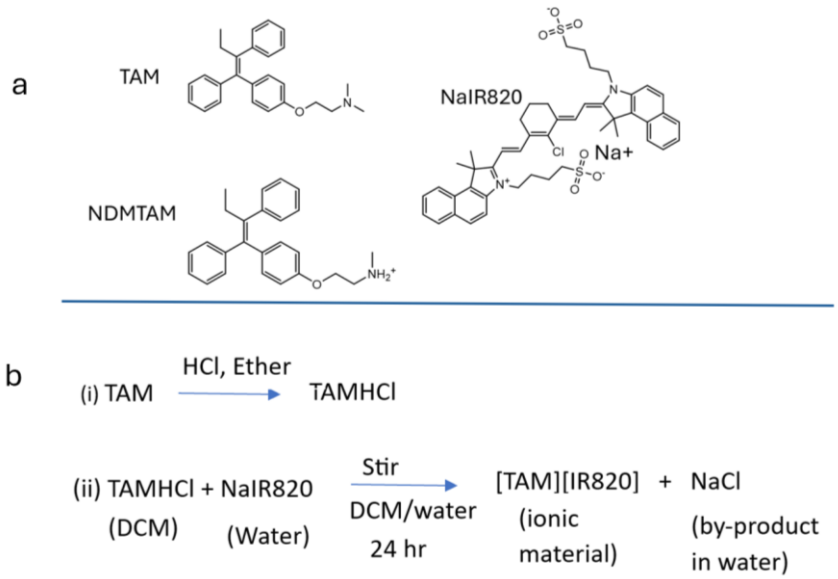

Figure 1. a) Structural formular of all chemo and photothermal drug b) Synthesis scheme for [TAM][IR820] Ionic material.

2.3 Synthesis and characterization of INMs

All INMs were prepared using a simple reprecipitation method in aqueous media (water or cell media) from IMs stock solution that was initially prepared in either ethanol or DMSO according to previously reported protocol.[17] Briefly, a dropwise addition of 1 mM stock solution (prepared in ethanol or DMSO) of the combination drug (IM) was introduced into a glass vial containing aqueous media in an active sonication bath. The content of the vial was sonicated for 5 mins and subjected to 15 mins rest period before any further measurement. For cellular studies, INMs were prepared in cell media. Whereas spectroscopic measurements were performed with INMs prepared in water from IMs in ethanol. The zeta potential and hydrodynamic diameter of the INMs prepared in DI water were determined using a Zetasizer pro red Malvern Instrument (Malvern Panalytical Limited, Westborough, MA) employing the dynamic light scattering method (DLS). Time dependent DLS size distribution and zeta potential of both INMs are reported in Table S1.

2.4 Photophysical properties

A UV-visible absorption spectrometer (Agilent Cary 5000, Santa Clara, CA) and a fluorometer (Horiba FluoroMax, Kyoto, Japan), were used to record the absorption and fluorescence emission spectra of the parent compounds, the synthesized IMs, and the INMs. Starna quartz cuvettes polished with two sides and a 10 mm pathlength were used for absorbance measurement. While for the fluorescence measurement, a starna quartz cuvette having four polished sides with 1 cm pathlength was used. All samples were measured at 826 nm excitation wavelength, same slit width, integration time of 0.1 s, and at right angle geometry.

2.5 Light to heat conversion efficiency

One important factor in selecting materials for photothermal therapy is the efficiency of PTA agent to convert absorbed light into heat. PTT dyes are commonly known for heat generation upon sufficient absorption of light. Determination of

a drug's photothermal effect requires the close monitoring of the dye's heating and cooling behavior upon laser irradiation overtime. To examine the PTT effect of the synthesized INMs, the drugs were prepared in cell media via simple reprecipitation method as previously stated in the nanoparticle synthesis (section 2.3). In a typical on-bench PTT experiment, a 1 mL (50 µM) solution of the NIR parent compounds or INMs was exposed to an 808 nm laser with 1 Wcm^{-2} power for 5 mins. A thermocouple probe was used to record the temperature of the solution for every 30 secs. This experiment was conducted for 5- 10 mins, with the first 5 mins to record the increasing temperature of the drug (laser turned off at the 5^{th} min) while the cooling temperature of the drug was recorded during the last 5 mins.

2.6 Reactive oxygen species (ROS) generation

Reactive oxygen species generation quantifies the photosensitizer's ability to produce ROS upon absorption of light. Since the 808 nm was used to investigate the light to heat conversion efficiency, it is quite possible that IR820 after absorption of laser light can undergo different routes as well such as photodynamic therapy (PDT). Photosensitizer like NaIR820 have been reported to induce ROS and exhibit some PDT effect.[16,17] Therefore, ROS production experiment were performed for the parent NIR dye and IMs separately to explore the changes in ROS production of the respective parent NIR dyes as compared to their chemo-PTT IMs. ROS experiment was performed by mixing a parent NIR dye solution or IM solution with DPBF probe solution prepared in ethanol. Briefly, NIR dye and DPBF were separately prepared in ethanol and equal volume of DPBF was added to the NIR dye solution separately to yield a resulting concentration of 10 µM drug in 200 µM DPBF. Upon irradiation of the mixture with IR 808 nm laser, the rate of ROS generation was determined by measuring the decrease in absorbance of DPBF probe at 411 nm after every 15 sec intervals for a period of 45 secs using the UV-Vis absorption spectrophotometer. NaIR820 was used as a standard for quantifying the ROS production of the parent NIR drugs and combination drug in ethanol according to Equation 1.

$$\Phi_{un} = \Phi_{std} \times \frac{S_{un}}{S_{std}} \times \frac{1 - 10^{-A_{std}}}{1 - 10^{-A_{un}}} \ldots\ldots\ldots\ldots\ldots Equation\ 1$$

where S represents the slope obtained from the plot of absorbance of the sample versus irradiation time, A is the absorbance of sample at the excitation wavelength in the absence of the probe, subscript '*un*' stands for the unknown samples analyzed, and subscript '*std*' represents the standard. Φ represents the ROS quantum yield.

2.7 Photostability measurements

A drug suitable for phototherapy should be highly photostable over the period of treatment. To investigate the photostability of the free NIR dyes or chemo-PTT combination drugs, 2 µM sample was prepared separately from ethanol stock and further subjected to fluorescence measurements in kinetic mode at interval of 0.1 sec over the course of 30 mins. Measurements were performed using a four-sided polished window quartz cuvette with 1 cm pathlength. Photostability measurement was performed at 826 nm excitation while excitation/emission slit widths were set for 14/14 nm.

2.8 Cellular uptake

Cellular uptake was designed based on previously reported protocol.[16,18] Cells at a seeding density of 1 x 10^6 cells per well were plated in a six well plate and incubated for 24 hr. Cells in each well were treated with 20 µM of parent NIR dyes or INMs prepared in cell media, with a total volume of 2.5 mL in each well and incubated for 6 or 8 hr. After allotted time, cells were washed thoroughly with PBS three times to eliminate any uninternalized drugs. Cells were then

lysed with 2.5 mL DMSO to expose the internalized drugs and then quantified by UV-Vis absorption spectrophotometer.

2.9 Cell viability studies

The cell viability of the drug is determined in the dark as well as under laser irradiation. For this experiment, MCF-7 cell lines were cultured in a monolayer at 37 ^{o}C and 5 % CO_2 in complete media. MCF-7 cells were grown in DMEM supplemented with FBS (10% v/v) and antibiotic solution containing penicillin/streptomycin (500 units/mL). Once the desired confluency is attained, the cells were trypsinized and stained with trypan blue exclusion dye, and then counted using a hemocytometer.

For dark cytotoxicity experiment, 1 x 10^4 cells per well were plated in 96-well plates and incubated for 24 hr in the dark at 37 ^{o}C with 5 % CO_2. Different concentrations of INMs were prepared by reprecipitating stock solution in DMEM media under sonication, while maintaining a sterile environment. After that, cells were treated with various INMs concentration for 48 or 72 hr. For an experiment involving the mixture of both therapeutic drug, both chemo drug and the PTA agent, i.e TAM.HCl or NDMTAM.HCl and NaIR820, (including their counterions- Cl^- and Na^+) were prepared separately in cell media. Next, the drugs were introduced (one after the other) in MCF-7 cells and incubated for 48 or 72 hr. To prevent cellular toxicity, the usage of DMSO was limited to a maximum of 0.5 percent. Each experiment was accompanied with complete media and DMSO controls. After the allotted time, uninternalized drugs were aspirated and the cells were washed with PBS prior to the determination of cell viability with MTT assay. A microplate reader (Biotek Synergy H1, Winooski, VT) was used to determine the optical density of MTT-formazan at 570 nm. Each in vitro experiment was performed in triplicate and repeated three times. Unless otherwise stated, all data showing error bars are presented as mean $\pm$ standard deviation (SD). The statistically significant difference in the mean values was determined using the two-tailed student "t" test. Values with significant difference are denoted as $*p < 0.05$, $**p < 0.01$, and $***p < 0.005$.

The light toxicity experiments were investigated to ascertain the phototherapeutic efficacy of the parent NIR dyes as well as the newly developed chemo-PTT INMs. For this experiment, 1 x 10^4 cells were seeded in alternating wells in a 96 well plate and incubated for 24 hr. Cells were further exposed to INMs or parent dyes prepared in cell media and incubated for 6 hr. After incubation, the drug containing media was aspirated and washed with PBS to eliminate excess drugs prior to replacement with the fresh cell culture media. Each well containing treatment was irradiated with a near-infrared laser (808 nm, 1 Wcm-2) for 5 mins. A similar control experiment with identical conditions was conducted alongside, but with no exposure to light. Upon completion of the irradiation, the well plate was incubated for an additional 24 hr before assessment of cell viability via MTT assay.

2.10 Cell death mechanism

Flow cytometry was conducted using PI (propidium iodide)/YO-PRO staining. Cells were plated at approximately 1 x 10^6 cells per well in a 6 well plate and incubated overnight. Next, cells were washed with PBS (pH 7.4) and treated with 20 µM INMs for 48 hr. After drug treatment, both floating and adherent cells were harvested by addition of 0.5 mL trypsin. Cells were further monitored closely for complete detachment under the microscope. This step was proceeded with trypsin's neutralization with 1 mL serum containing media. The cells mixture was then transferred into a centrifuge tube and spun for 5 mins at 1100 RPM. Following a 5 min centrifugation, the cell pellet was washed with cold PBS and re-centrifuged again for an additional 5 mins. In accordance with the manufacturer's protocol, 1 µL of PI

and YO-PRO solutions were added to the cells that were resuspended in 0.25- 0.5 mL PBS in flow cytometry tubes. The tubes containing cells were kept in ice-bath and proceeded for flow cytometry data collection.

3. RESULTS AND DISCUSSION

3.1 IMs Characterization

IR820- based IMs were characterized in detail to investigate the presence of cation and anion in the combination drugs as well as the purity of the compound. Both synthesized IMs, i.e [TAM][IR820] and [NDMTAM][IR820] were characterized using ESI-MS. The mass-to charge ratio peaks in the positive and negative ion mode confirmed the presence of both the cation and anion in the [TAM][IR820] and [NDMTAM][IR820] IMs. An expected m/z^+ peak of 371.5 was calculated for TAM cation which is observed in positive ion mode with an experimental value of m/z^+ peak at 372.2 for [TAM][IR820]. In negative mode, the experimental m/z^- peak for IR820 at 825.3 corresponds to a calculated value of 826.4 for [TAM][IR820].

Similarly, for [NDMTAM][IR820] IMs, an expected m/z^+ peak of 357.5 was calculated for NDMTAM cation which is observed in positive ion mode with an experimental value of m/z^+ of 358.2. In negative ion mode, the experimental m/z^+ peak at 825.2 correlates with the calculated value of 826.4 for [NDMTAM][IR820]. Mass spectra data for all compounds are shown in Figure S2 (SI). These IMs were further characterized using ^{1}H- NMR. NMR spectra are presented in Figure S3 in SI.

3.2 INMs characterization

All INMs were characterized using dynamic light scattering (DLS) measurements to examine the solvated diameter of the nanoparticles. The observed sizes for all INMs are summarized in Table S1 (SI). Zeta potential measurements were also performed using Zetasizer pro red Malvern instrument to determine the surface charge of the particles, and the results are also presented in Table S1. It was observed that the [TAM][IR820] INMs and [NDMTAM][IR820] INMs exhibited a negative surface charge.

3.3 Photophysical properties

Photophysical properties of all parent NIR compounds, newly developed IMs and INMs were all carefully investigated in water and ethanol. The observed alterations in the absorption and fluorescence emission spectra of all combination drugs in both solvents were recorded and compared with respective parent compounds.

In ethanol, NaIR820, [TAM][IR820] and [NDMTAM][IR820] all exhibited similar absorption spectra with the absorbance maxima wavelength recorded at 826 nm along with a shoulder peak around 750 nm (Figure 2a). In addition, the molar absorptivity of IR820 anion increased in both [TAM][IR820] and [NDMTAM][IR820] IMs in comparison to NaIR820 in ethanol. In water, all the three compounds showed a broader spectrum that absorbs a wide range of wavelengths of electromagnetic radiation. NaIR820 showed absorption spectra with two peaks at 688 nm and 817 nm. Interestingly, a red shift was observed at both peaks for [TAM][IR820] and [NDMTAM][IR820] INMs in water from 688 nm to 735 nm and from 817 nm to 835 nm. A bathochromic shift as well as a broader spectrum (Figure 2b) was observed for both INMs that demonstrate a longer wavelength NIR absorption of light by INMs which is highly desirable for deeper penetration of tissues to treat deep seated tumors. It was also observed that both INMs exhibited a higher molar absorptivity value as compared to the parent NaIR820 in water as reported in Table S2.

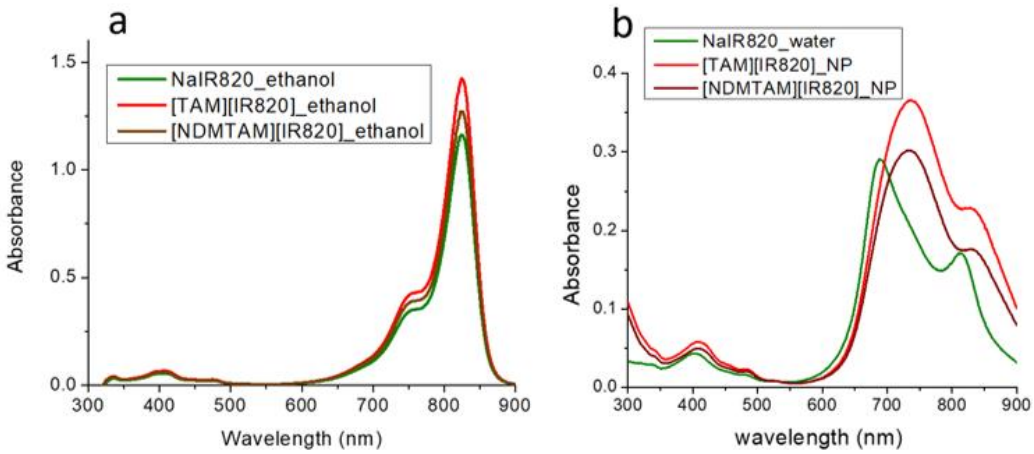

Figure 2: Absorption spectra of 5 µM of [TAM][IR820], [NDMTAM][IR820] INMs and NaIR820 compound in a) ethanol b) water.

Fluorescence emission spectra of NaIR820 parent compound, derived chemo-PTT IMs and INMs samples are presented in Figure 3. When IMs were excited at 750 nm wavelength, the fluorescence emission intensity of [TAM][IR820] IM in ethanol was found to increase slightly as compared to the parent NaIR820 dye as shown in Figure 3a. There were no significant changes in the fluorescence emission spectra for both [NDMTAM][IR820] and NaIR820 in ethanol. In contrast, when the INMs were excited at 750 nm wavelength, both [TAM][IR820] and [NDMTAM][IR820] INMs depicted a tremendous decrease in fluorescence emission intensity when compared with NaIR820 parent compound in water (Figure 3b). Similarly, there were no alterations in the fluorescence emission wavelength except with a decrease in their fluorescence intensity when compared with their respective parent compound. A decrease in the fluorescence emission intensity for both INMs is expected due to the nanoparticle formation as opposed to the soluble drugs prepared in ethanol. Another excitation wavelength experiment was designed to investigate the effect of excitation wavelength. This is to investigate any potential alterations in their fluorescence spectra when excited at either the shoulder peak or the absorbance maximum wavelengths (Figure 3c and d). In ethanol, NaIR820 parent compound exhibited the highest fluorescence intensity as compared to both IMs. However, in water a similar trend existed for NaIR820 with the highest fluorescence intensity as opposed to both [TAM][IR820] and [NDMTAM][IR820] INMs. This decrease in fluorescence emission intensity in TAM base INMs is indicating the possibility of non-radiative rate.[16] Therefore, we expect that INMs are more suitable as a photothermal agent as compare to the soluble IR820.

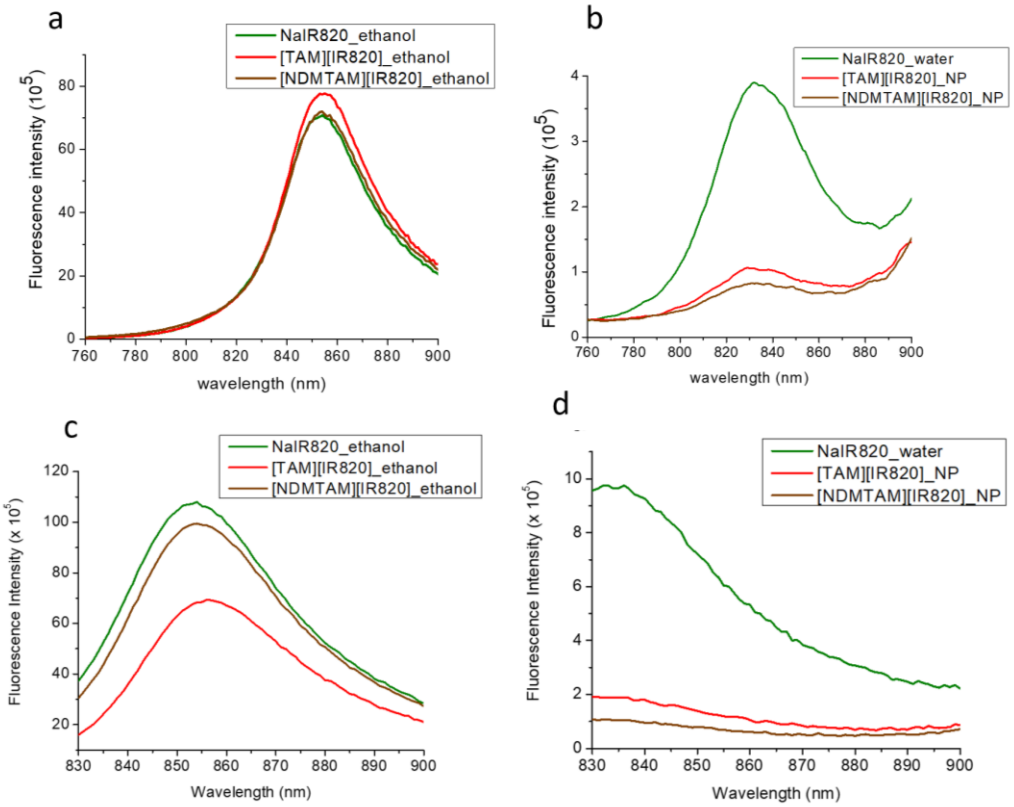

Figure 3: Fluorescence emission spectra of [TAM][IR820], [NDMTAM][IR820] IMs and parent NaIR820 compound in a) ethanol at 750 nm excitation wavelength b) water at 750 nm excitation wavelength c) ethanol at 820 nm excitation wavelength d) water at 820 nm excitation wavelength. Sample concentration of 5 µM.

3.4 Photostability

The photostability of all PTAs were investigated by recording the fluorescence emission of the drug over a period of 30 mins while continually exposed to radiation at their respective excitation wavelengths. In this experiment, the slit width was set to 14/14 nm. The photostability results (Figure S4) for NaIR820 parent compound, derived chemo-PTT IMs, and INMs showed that all the compounds are photostable within the period of study.

3.5 Light to heat conversion efficiency

Heat generated by a PTA upon absorption of light is quantified by the light to heat conversion efficiency. NIR dyes are known as potential photothermal therapy candidates. Hence, it is necessary to analyze the alterations in the PTT behavior of the parent NaIR820 dye when converted to INMs upon exposure to IR 808 nm laser. The light to heat conversion efficiency of parent NaIR820 compound and derived chemo-PTT INMs were measured in cell media. Light to heat conversion efficiency graphs for the PTA and INMs in cell media are reported in Figure 4. From the light to heat conversion curves, it was observed that the temperature of INMs or PTA generally enhanced with increasing irradiation time as compared to the control (cell media). This signifies that the INMs as excellent PTAs that convert the absorbed 808 nm laser light to heat energy. The light to heat conversion efficiency were computed using the light to heat conversion efficiency Equations S1-S4 (SI), with the summarized results reported in Table 1. Light to heat conversion efficiency results showed that both [TAM][IR820] and [NDMTAM][IR820] INMs performed better as compared to the parent NaIR820. The result reported in Table 2 demonstrated that the PTT activity of the NIR dye was improved upon conversion to INM. An increase in the light to heat conversion efficiency of both [TAM][IR820] and

[NDMTAM][IR820] INMs in comparison to NaIR820 parent compound validated the enhancement of non-radiative transition as observed by the decreased fluorescence emission (Figure 3b and d). In essence, the lower fluorescence emission exhibited by both INMs depicts that the compound (upon absorption of light) preferably relaxes to ground state by generating heat. This signifies the importance of nanoparticle morphology which is essential to attain high phototherapeutic effect by a photosensitizer.

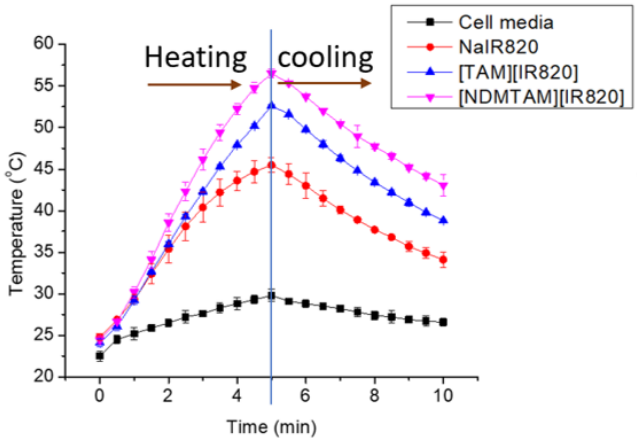

Figure 4: Light to heat efficiency curve for NaIR820, [TAM][IR820] and [NDMTAM][IR820] INMs in cell media. Error bars are presented as mean ± standard deviation (SD).

Table 1: Photothermal efficiency (η) for both INMs and parent dyes in different media.

Drugs	η in cell media (%)
NaIR820	13.51
[TAM][IR820]	16.96
[NDMTAM][IR820]	14.63

3.6 ROS generation

Since PTA drugs have also been reported to generate ROS,[16–18] the reactive oxygen quantum yield was investigated to further elucidate the other light mediated mechanism that the IR820 based drug can utilize after absorption of the 808nm laser light. ROS quantification experiment was designed to determine the photodynamic activity of IMs in the presence of TAM and NDMTAM counterions. ROS quantum yields of NaIR820 parent compound and derived chemo-PTT IMs were determined in the presence of a commonly used molecular probe (DPBF) that scavenges ROS. In the presence of ROS, the yellow coloration of DPBF turns colorless (1,2-dibenzoyl benzene), and the ROS generation is quantified by recording the rate of decrease in absorbance of DPBF upon irradiation at the wavelength maxima of the photosensitizer.[16,18] Figure S5 shows the decrease in DPBF absorbance upon increasing irradiation time in the presence of the [TAM][IR820] IM. A control experiment investigating the photostability of DPBF only, has been previously reported by our group to show that ROS is not produced by DPBF except in the presence of a photosensitizer.[17] The ROS quantum yield was calculated using Equation 1, and the slope was calculated from the graph shown in Figure S6. ROS quantum yield results for both IMs exhibited a slight increase as compared to the parent soluble drug (Table S3). This slight enhancement of the PDT activity of IR820 is attributed to the presence of the TAM and NDMTAM counter anion. Thus, it is validated that counterion can affect PTT and PDT activity of a photosensitizer. Upon comparing the PDT and PTT results, the PTT activity is more dominant as compared to PDT mechanism. Thus, the tumor will be mainly ablated by the PTT mechanism and slightly eradicated by the PDT mechanism in these TAM based combination INMs.

3.7 Cellular uptake

Cellular uptake of both INMs and parent NaIR820 soluble compound were investigated overtime in MCF-7 breast cancer cells to examine the effect of the nanodrug's morphology in comparison to the soluble free NIR dye. The time dependent cellular uptake of NaIR820 soluble parent NIR dye and INMs in MCF-7 cells are reported in Figure S7 (SI). Nanoparticles are known to be greatly accumulated within the tumor as opposed to the soluble drugs due to EPR effect.[19] This is evident by the increased concentration of the INMs in MCF-7 cells as compared to the parent drug as shown in Figure S7 (SI). The soluble parent dye or INMs internalized by the cells was quantified using a UV-Visible spectrophotometer. It was observed that the cellular uptake of [NDMTAM][IR820] and [TAM][IR820] INMs was significantly increased in comparison to NaIR820 parent compound for the duration of study. Further examination of the cellular uptake of the drugs revealed a slight decrease in the uptake for both [TAM][IR820] and [NDMTAM][IR820] INMs in MCF-7 cells overtime. This could be attributed to the nanoparticle morphology of the INMs (Figure S7). The highest uptake was observed for [NDMTAM][IR820] as compared and [TAM][IR820] INMs which is attributed to the size of [NDMTAM][IR820] INM.

3.8 In vitro cellular dark toxicity of INMs

In vitro cytotoxicity is determined to examine the performance of the combination drugs (INMs) with respect to the chemotherapeutic or photothermal NIR dyes separately. First the dark toxicity of the INMs and their parent compound were evaluated. Our group have previously examined the dark cytotoxic response of NaIR820 towards MCF-7 cells, and it was completely nontoxic to MCF-7 cells at a concentration range below 20 μM.[16] Whereas, TAM and NDMTAM, the chemotherapeutic drugs are known to be cytotoxic towards cancerous cells and their cytotoxicity increases when exposed to cells for longer period of time.[3,5,11] In this work, TAM IC_{50} decreased over time but no change in IC_{50} was observed for NDMTAM. Therefore, it is crucial to understand how the chemotherapeutic activity changes in the presence of the NIR dye counteranions. In vitro cytotoxicity of all drugs was investigated at 48 and 72 hr. Figure 5a and b shows the dark cytotoxicity results for all TAM and NDMTAM-based derivatives investigated for 48 and 72 hr, respectively. The summarized IC_{50} results for all INMs are also reported in Table 2. Examination of the dark plate results revealed that [TAM][IR820] INMs showed an enhanced cytotoxic performance towards MCF-7 cells as compared to the parent chemotherapeutic drug (TAM). The IC_{50} value is almost half for 72 hr cell viability study. [NDMTAM][IR820] INMs also exhibited an increased cytotoxic response in relation to NDMTAM due to the nanoparticle morphology and enhanced cellular uptake. Furthermore, examination of the dark cytotoxicity results for both TAM, NDMTAM and their respective INMs chemotherapeutic drug revealed that there was no significant difference in their IC_{50} value but TAM is slightly more toxic than NDMTAM. These results could possibly signify that the absence of the methyl group in the NDMTAM as opposed to TAM did not significantly impact the cytotoxic performance of the drugs towards MCF-7 cells.

To further understand the significance of ionic liquid chemistry used for the development of the INMs (combination drug), a dark cytotoxicity experiment was designed using a mixture of both soluble parent drug (TAM chemo parent and NaIR820) in MCF-7 cells. This experiment was aimed to unveil the therapeutic efficacy of the INMs as opposed to treatment involving separate addition of both soluble chemo and PTT drug without removal of sodium chloride counterions. For this study, a similar dark cytotoxicity experimental procedure was employed. Both chemo drug and the PTA agent, i.e TAM.HCl or NDMTAM.HCl and NaIR820, (including their counterions- Cl^- and Na^+) were prepared separately in cell media. Next, the drugs were introduced (one after the other) in MCF-7 cells and incubated for 48 or

72 hr. Figure S8 shows the cell viability graph for both therapeutic agents added in the parent forms. The cell viability results for the mixture of two parent compounds (soluble drugs) showed lesser cytotoxic effect (increased IC_{50}) towards MCF-7 cells as compared to the treatment with the INMs (Table 2). The decreased cytotoxic response exhibited by the mixture of parent compounds treatment is possibly attributed to the lower uptake of soluble drugs. It is worth pointing out that the soluble drugs mixture could not perform well possibly due to the presence of Na^+ and Cl^- counterions. However, the INMs are completely free from Na^+ and Cl^- (removed during IM synthesis) and their enhanced cytotoxicity could be ascribed to their nanoparticle morphology, increased cellular uptake, and enhanced EPR effect towards the tumor cells.

To further elucidate the effect of the presence of the NIR dyes incorporated to the chemotherapeutic drug in the nanoparticle form, it is crucial to investigate the photothermal effect of the drugs in the presence of NIR light irradiation. Therefore, the newly developed INMs were subjected to light irradiation in vitro.

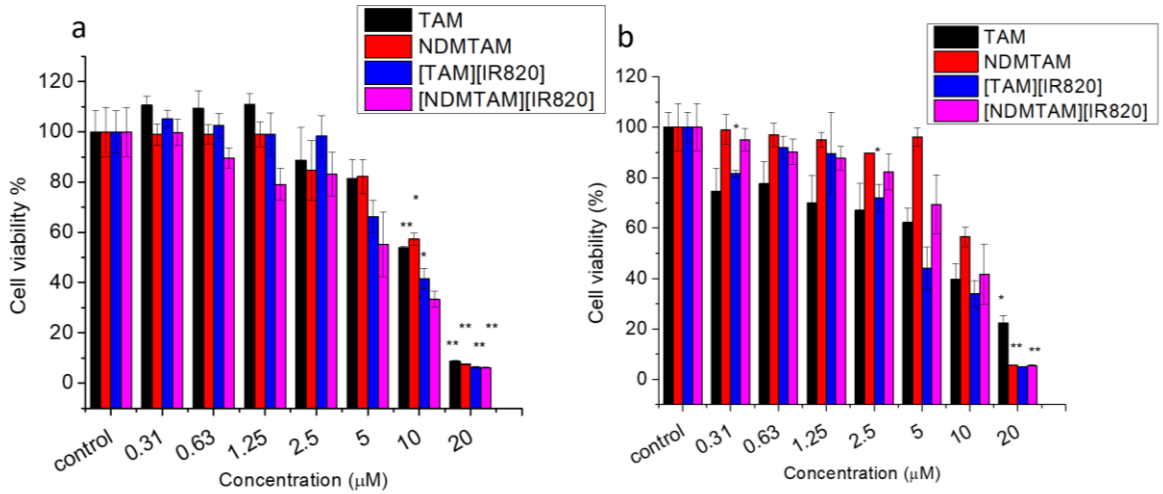

Figure 5: Dark cytotoxicity results for TAM, NDMTAM parent compounds, TAM and NDMTAM-based INMs in MCF-7 cancer cells at various concentrations for a) 48 hr and b) 72 hr drug incubation. p values are determined using two-tailed student's t-test and are reported as *p< 0.05, **p< 0. 01, ***p< 0.005.

Table 2: Cell viability results (dark study) for all parent drugs, INMs and mixture of the soluble parent compounds in MCF-7 cells (μM).

Drug (INMs)	IC_{50} values (dark study-48 hr)	IC_{50} values (dark study-72 hr)
TAM	10.2 ± 0.3	9.6 ± 0.55
[TAM][IR820]	7.3 ± 2.05	4.8 ± 1.1
NDMTAM	10.7 ± 1.5	10.7 ± 1.2
[NDMTAM][IR820]	7.5 ± 0.6	6.8 ± 1.2
TAM.HCl + NaIR820	15.2 ± 1.3	11.1. ± 0.05
NDMTAM.HCl + NaIR820	12 ± 0.5	10.3. ± 0.1

3.9 In vitro photo-thermal effects of INMs

Light cytotoxicity is determined to assess the photothermal cytotoxic response of the chemo-PTT combination drugs as opposed to the parent NaIR820 dye. According to the on-bench light-to-heat conversion efficiency data, the INMs effectively generated heat in the cell medium. Therefore, in vitro PTT capability of the drugs was examined in the presence of NIR 808 nm laser. For this experiment, MCF-7 cells were subjected to 6 hr of drug incubation, followed by

light irradiation. We have previously investigated the light cytotoxicity of NaIR820 dyes on MCF-7 cells.[16] Figure 6 and Table 3 shows the light cytotoxic results for NaIR820, TAM and NDMTAM-based INMs towards MCF-7 cells. It was observed that only [TAM][IR820] and [NDMTAM][IR820] INMs exhibited a higher light cytotoxicity response as compared to the parent free dye. This is evident from the lowered IC_{50} value. The increased cytotoxic effect of both IR820 based INMs is attributed to their nanoparticle morphology, enhanced cellular uptake, weak fluorescence emission intensity, their improved ROS quantum yield and light to heat conversion efficiency. Similar light experiment was performed for the mixture of both soluble parent drugs to MCF-7. The result from the light plate indicated that the INMs exhibited increased cytotoxic response (Figure 6) in comparison to the mixture of parent soluble drugs (Figure S9) due to the nanoparticle morphology and cellular uptake of the particles in MCF-7 cells. The outcomes of the experiments on the cytotoxicity of the INMs under light and dark led to the curiosity to investigate the interaction or relationship between the chemotherapeutic and photothermal moiety. Thus, the combination index of the chemo-PTT combination INMs and the mixture involving two parent soluble drugs was calculated.

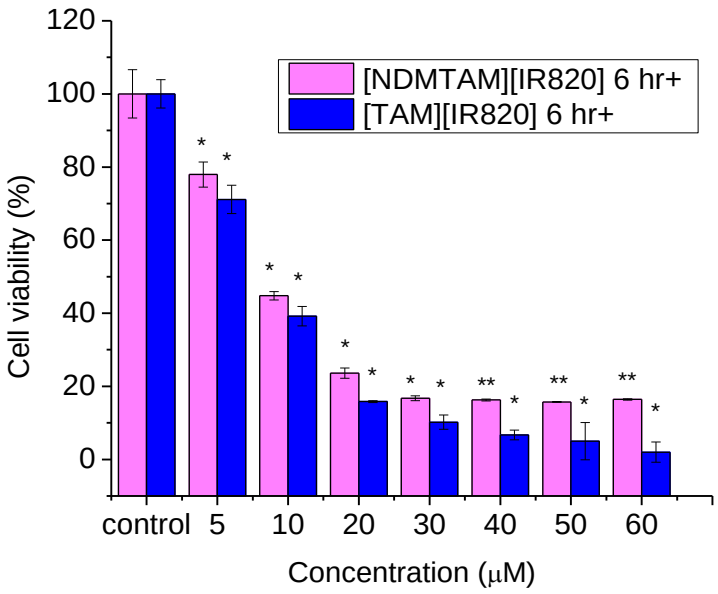

Figure 6: Photo cytotoxicity of TAM and NDMTAM-based INMs in MCF-7 cancer cells incubated for 6 hr followed by 5 min irradiation with 808 nm laser (1 Wcm^{-2}). p values are determined using two-tailed student's t-test and are reported as *p< 0.05, **p< 0.01, ***p< 0.005.

Table 3: Cell viability results for light study on MCF-7 (μM).

Drug (INMs)	IC_{50} Values (Light study 6 hr+)
[TAM][IR820]	7.56 ± 0.99
[NDMTAM][IR820]	9.10 ± 1.05
NaIR820 [16]	24.01 ± 0.99
TAM.HCl + NaIR820	28.7 ± 0.5
NDMTAM.HCl + NaIR820	24.03 ± 0.3

3.10 Combination Index (CI)

Since our chemo-PTT combination INMs are composed of both chemo and photothermal agents, their degree of interaction can be investigated using the combination index (CI). The Chou-Talalay method[20] was used to examine the degree of interaction of drug combinations, as shown in Equation 2. A CI value ranging from 0.90-1.10, 0-0.99, and

greater than 1.1 represents a nearly additive, synergistic and an antagonistic interaction. If both medications have an additive effect, the specific negative effects of one medication can be lessened while still achieving the same level of therapeutic efficacy.

$$CI = \frac{IC50\ (A+B)}{IC50(A)} + \frac{IC50\ (A+B)}{IC50(B)} - - - - Equation\ 2$$

Where IC_{50} (A+B) represents the IC_{50} value for chemo-PTT combination drug and IC_{50} A or B represents IC_{50} value of chemotherapeutic drug and PTT drug respectively.

In this case, the chemo and photothermal agent represents A and B, respectively. It was observed that both [TAM][IR820] and [NDMTAM][IR820] INMs had CI of 1.03 and 1.07 for the 48 hr study, indicating a nearly additive combination of the two therapies. Interestingly the CI was slightly lower for [TAM][IR820] INMs when investigated at longer time (72 hr) that depict the great synergy between chemo and PTT drugs. Table 4 shows the CI for all treatments involving INMs as well as the mixture of two parent drugs at different time. The CI result revealed an additive effect for INMs (CI value nearly 1), and an antagonistic interaction between parent chemo and NaIR820 mixture as the soluble drugs (CI value above 1). This result answers the lower toxicity of the parent compound mixtures in vitro study. Examination of results revealed that ionic liquid chemistry is significantly enhancing the synergism between two drugs thus it is important to develop combination drugs using ionic liquid chemistry and remove the spectator counterions. In addition, the cytotoxicity of both chemo and PTT mechanisms in combination INMs are improved in the absence of FRET phenomenon. Thus, it further validates that ionic liquid chemistry to develop combination nanomedicines is a promising strategy to attain enhanced therapeutic efficiency. This study is designed to validate the ionic liquid chemistry and presence/absence of FRET mechanism; Thus, no other cell lines were tested.

Table 4: Combination index for all the chemo-PTT combination INMs and the independent treatment involving parent soluble drugs.

Drugs	CI for 48 hr study	CI for 72 hr study
[TAM][IR820]	1.03	0.815
[NDMTAM][IR820]	1.07	1.01
TAM.HCl + NaIR820	2.68	1.79
NDMTAM.HCl + NaIR820	2.12	1.33

3.11 Cell death mechanism

The enhanced cytotoxicity results directed us to design a new experiment about the cell death mechanism. A quantitative analysis like flow cytometry is useful for determining the mode of cell death such as apoptosis or necrosis. Flow cytometry results are shown in Figure 7a-e. Total apoptosis cell death was determined by adding up the percentage of cells undergoing both early and late apoptosis. As evident from the flow cytometry results, total apoptotic response of parent TAM was about 5.2 % which is also very similar to the apoptotic signal recorded with cells treated with NDMTAM (5.5 %). This is consistent with the previously reported cytotoxicity results of TAM-based drugs (Table 2). It is very important to investigate the cell death mechanism of newly developed INMs since these they exhibited improved cytotoxicity. Interestingly, the apoptotic signal for both [TAM][IR820] and [NDMTAM][IR820] INMs was significantly enhanced when the parent chemotherapeutic drugs were modified to nanoparticles. For treatment involving [NDMTAM][IR820] INMs, the percentage apoptosis was increased by three times (16.6 %) in relation to the parent NDMTAM (5.5 %). More significantly, a greater percent apoptosis signal of 38.5 % was observed

for [TAM][IR820] INMs in dark. This represents more than seven-times increase in the apoptotic signal response in comparison to TAM's. It demonstrated that NIR counteranions impacted the TAM's efficacy and led to an accelerated apoptotic cell death mechanism. Moreover, the notable apoptotic response from both INMs was also attributed to enhanced EPR effect of the nanodrugs inside the tumor. Therefore, it is important to highlight that IM chemistry strategy enhanced the potency of TAM and its metabolites, NDMTAM without any FRET mechanism.

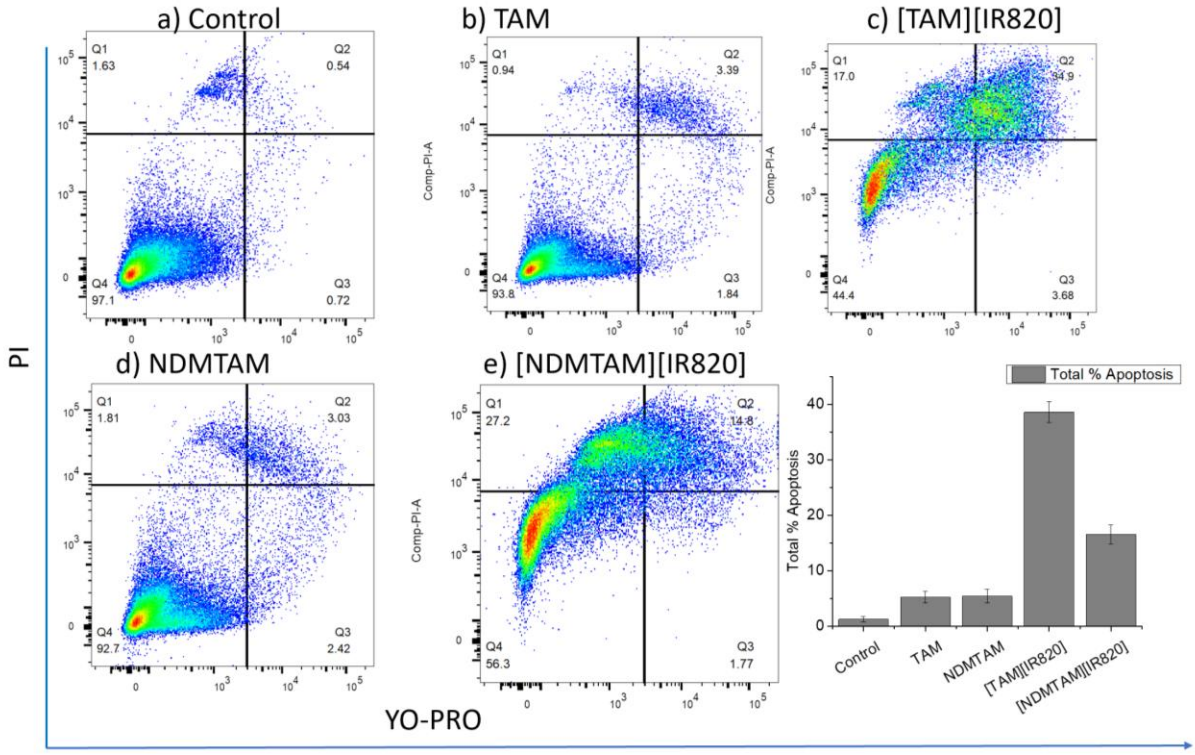

Figure 7: a-e) Flow cytometry results using YO-PRO/propidium-iodide (PI) staining of MCF-7 cells treated separately with 20 µM TAM, NDMTAM parent compound, [TAM][IR820], and [NDMTAM][IR820] INMs after 48 hr drug incubation. Numbers in quadrants show percentages (%) of total cell populations. Data from flow cytometry experiments were represented here in the form of bar graphs. Error bars are presented as mean ± standard deviation (SD).

4.0 CONCLUSION

Two distinct tamoxifen and N-desmethyl TAM based NIR IMs were successfully developed using the ionic liquid chemistry strategy via a simple ion exchange reaction. Then, carrier-free INMs were directly prepared from the IMs via a simple reprecipitation method. Detailed photophysical characterization of both nanodrug signifies their potential to be clinically relevant due to their tendency to absorb longer wavelength electromagnetic radiation. On bench photothermal investigation of both TAM and NDMTAM-based ionic nanomedicines revealed improved light-to-heat conversion efficiencies as opposed to their respective parent compounds. In addition, both nanodrugs also showed an increase in ROS quantum yield as compared to the parent NIR dye with [NDMTAM][IR820] exhibiting a greater degree of PDT activity. Cellular uptake results also depicted that MCF-7 cells had increased uptake for both [TAM][IR820] and [NDMTAM][IR820] nanoparticles as opposed to the soluble NIR dye. In vitro light and dark cytotoxicity was also enhanced significantly for both INMs as opposed to the parent chemo, NIR dye and the mixture of two parent soluble drugs. Degree of interaction were obtained to be mostly additive for both TAM and NDMTAM-based ionic

nanomedicines as opposed to the treatment involving mixture of parent drugs which exhibited antagonistic behavior. Interestingly, both INMs exhibited an increased apoptosis cell death mechanism (more than three-seven times) in relation to the parent chemotherapeutic drugs. Collectively, these observations suggests that INMs strategy can be used to better enhance the potency of TAM and NDMTAM chemotherapeutic drugs. Additionally, both [TAM][IR820] and [NDMTAM][IR820] INMs have the potential to be used as chemo-PTT combination drugs even though they lack FRET capabilities.

Supporting Information

The supporting information is available within this main manuscript.

Author Contribution

M.B., M.F., S.M., N.S.: Conceptualization. M.B., M.F., N.S.: Data curation. M.B., M.F., S.S., A.O.: Formal analysis. N.S.: Funding acquisition. M.B., M.F., S.S., A.O.: Investigation. M.B., N.S.: Methodology. M.B., N.S.: Project administration. M.B., M.F., N.S.: Resources. N.A., N.S.: Supervision. M.B., M.F., S.S., N.S.: Validation. M.B., N.A., R.G., A.K.O., N.S.: Visualization. M.B., Writing. M.B., N.A., R.G., A.K.O., N.S.: Writing-review & editing.

Notes

The authors declare no competing financial interest.

ACKNOWLEDGEMENTS

This publication was made possible by the Arkansas INBRE program, supported by a grant from the National Institute of General Medical Sciences, (NIGMS), P20 GM103429 from the National Institutes of Health. N.S. gratefully acknowledges financial support through the National Science Foundation EPSCoR Research Infrastructure under award number RII Track 4-1833004. Any opinions, findings, and conclusions or recommendations expressed in this material are those of the author(s) and do not necessarily reflect the views of the National Institute of Health or the National Science Foundation.

REFERENCES

1. Ağardan, N. B. M.; Değim, Z.; Yılmaz; Altıntaş, L.; Topal, T. Tamoxifen/Raloxifene Loaded Liposomes for Oral Treatment of Breast Cancer. *J. Drug Deliv. Sci. Technol.* **2020**, *57* (December 2018). https://doi.org/10.1016/j.jddst.2020.101612.
2. Goldstein, S. R.; Siddhanti, S.; Ciaccia, A. V.; Plouffe, L. A Pharmacological Review of Selective Oestrogen Receptor Modulators. *Hum. Reprod. Update* **2000**, *6* (3), 212–224. https://doi.org/10.1093/humupd/6.3.212.
3. Theodossiou, T. A.; Ali, M.; Grigalavicius, M.; Grallert, B.; Dillard, P.; Schink, K. O.; Olsen, C. E.; Wälchli, S.; Inderberg, E. M.; Kubin, A.; Peng, Q.; Berg, K. Simultaneous Defeat of MCF7 and MDA-MB-231 Resistances by a Hypericin PDT–Tamoxifen Hybrid Therapy. *npj Breast Cancer* **2019**, *5* (1). https://doi.org/10.1038/s41523-019-0108-8.
4. Morad, S. A. F.; Madigan, J. P.; Levin, J. C.; Abdelmageed, N.; Karimi, R.; Rosenberg, D. W.; Kester, M.; Shanmugavelandy, S. S.; Cabot, M. C. Tamoxifen Magnifies Therapeutic Impact of Ceramide in Human Colorectal Cancer Cells Independent of P53. *Biochem. Pharmacol.* **2013**, *85* (8), 1057–1065. https://doi.org/10.1016/j.bcp.2013.01.015.
5. Shagufta; Ahmad, I. Tamoxifen a Pioneering Drug: An Update on the Therapeutic Potential of Tamoxifen

Derivatives. *Eur. J. Med. Chem.* **2018**, *143*, 515–531. https://doi.org/10.1016/j.ejmech.2017.11.056.

6. Greenberger, L. M.; Annable, T.; Collins, K. I.; Zhang, Y.; Frost, P.; Komm, B. S.; Lyttle, C. R.; Miller, C. P.; Satyaswaroop, P. G. A New Antiestrogen, 2-(4-Hydroxy-Phenyl)-3-Methyl-1-[4-(2-Piperidin-1-Yl-Ethoxy)-Benzyl]-1H- Indol-5-Ol Hydrochloride (ERA-923), Inhibits the Growth of Tamoxifen-Sensitive and -Resistant Tumors and Is Devoid of Uterotropic Effects in Mice and Rats. *Clin. Cancer Res.* **2001**, *7* (10), 3166–3177.
7. Ignatov, A.; Ignatov, T.; Roessner, A.; Costa, S. D.; Kalinski, T. Role of GPR30 in the Mechanisms of Tamoxifen Resistance in Breast Cancer MCF-7 Cells. *Breast Cancer Res. Treat.* **2010**, *123* (1), 87–96. https://doi.org/10.1007/s10549-009-0624-6.
8. Ma, J.; Guo, Y.; Chen, S.; Zhong, C.; Xue, Y.; Zhang, Y.; Lai, X.; Wei, Y.; Yu, S.; Zhang, J.; Liu, W. Metformin Enhances Tamoxifen-Mediated Tumor Growth Inhibition in ER-Positive Breast Carcinoma. *BMC Cancer* **2014**, *14* (1), 1–11. https://doi.org/10.1186/1471-2407-14-172.
9. Costa, A.; Scholer-Dahirel, A.; Mechta-Grigoriou, F. The Role of Reactive Oxygen Species and Metabolism on Cancer Cells and Their Microenvironment. *Semin. Cancer Biol.* **2014**, *25*, 23–32. https://doi.org/10.1016/j.semcancer.2013.12.007.
10. Greten, F. R.; Grivennikov, S. I. Inflammation and Cancer: Triggers, Mechanisms, and Consequences. *Immunity* **2019**, *51* (1), 27–41. https://doi.org/10.1016/j.immuni.2019.06.025.
11. Christodoulou, M. S.; Fokialakis, N.; Passarella, D.; García-Argáez, A. N.; Gia, O. M.; Pongratz, I.; Dalla Via, L.; Haroutounian, S. A. Synthesis and Biological Evaluation of Novel Tamoxifen Analogues. *Bioorganic Med. Chem.* **2013**, *21* (14), 4120–4131. https://doi.org/10.1016/j.bmc.2013.05.012.
12. Li, Q.; Zhao, G.; Wu, F.; Tang, X.; Liao, Z.; Liang, X.; Dong, W. Imperatorin-Loaded RH60 / MPEG − PLLA Micelles for Reversing Tamoxifen Resistance in Breast Cancer. **2023**. https://doi.org/10.1021/acsanm.3c04185.
13. Jiang, Q.; Zheng, S.; Wang, G. Development of New Estrogen Receptor-Targeting Therapeutic Agents for Tamoxifen-Resistant Breast Cancer. *Future Med. Chem.* **2013**, *5* (9), 1023–1035. https://doi.org/10.4155/fmc.13.63.
14. Jang, S. Y.; Kim, A.; Kim, J. K.; Kim, C.; Cho, Y. H.; Kim, J. H.; Kim, C. H.; Lee, J. Y. Metformin Inhibits Tumor Cell Migration via Down-Regulation of MMP9 in Tamoxifen-Resistant Breast Cancer Cells. *Anticancer Res.* **2014**, *34* (8), 4127–4134.
15. Li, C.; Wang, Y.; Zhang, S.; Zhang, J.; Wang, F.; Sun, Y.; Huang, L.; Bian, W. PH and ROS Sequentially Responsive Podophyllotoxin Prodrug Micelles with Surface Charge-Switchable and Self-Amplification Drug Release for Combating Multidrug Resistance Cancer. *Drug Deliv.* **2021**, *28* (1), 680–691. https://doi.org/10.1080/10717544.2021.1905750.
16. Bashiru, M.; Macchi, S.; Forson, M.; Khan, A.; Ishtiaq, A.; Oyebade, A.; Jalihal, A.; Ali, N.; Griffin, R. J.; Oyelere, A. K.; Hooshmand, N.; Siraj, N. Doxorubicin-Based Ionic Nanomedicines for Combined Chemo-Phototherapy of Cancer. *ACS Appl. Nano Mater.* **2024**, *7* (2), 2176–2189. https://doi.org/10.1021/acsanm.3c05464.
17. Macchi, S.; Jalihal, A.; Hooshmand, N.; Zubair, M.; Jenkins, S.; Alwan, N.; El-Sayed, M.; Ali, N.; Griffin, R. J.; Siraj, N. Enhanced Photothermal Heating and Combination Therapy of NIR Dye via Conversion to Self-Assembled Ionic Nanomaterials. *J. Mater. Chem. B* **2022**, *10* (5), 806–816. https://doi.org/10.1039/D1TB02280F.
18. Forson, M.; Bashiru, M.; Macchi, S.; Singh, S.; Anderson, A. D.; Sayyed, S.; Ishtiaq, A.; Griffin, R.; Ali, N.; Oyelere, A. K.; Berry, B.; Siraj, N. Cationic Porphyrin-Based Ionic Nanomedicines for Improved Photodynamic Therapy. *ACS Appl. Bio Mater.* **2023**, *6* (12), 5662–5675. https://doi.org/10.1021/acsabm.3c00809.

19. Li, R.; Zheng, K.; Yuan, C.; Chen, Z.; Huang, M. Be Active or Not: The Relative Contribution of Active and Passive Tumor Targeting of Nanomaterials. *Nanotheranostics* **2017**, *1* (4), 346–357. https://doi.org/10.7150/ntno.19380.
20. Chou, T. C. Theoretical Basis, Experimental Design, and Computerized Simulation of Synergism and Antagonism in Drug Combination Studies. *Pharmacol. Rev.* **2006**, *58* (3), 621–681. https://doi.org/10.1124/pr.58.3.10.

Supplementary Information

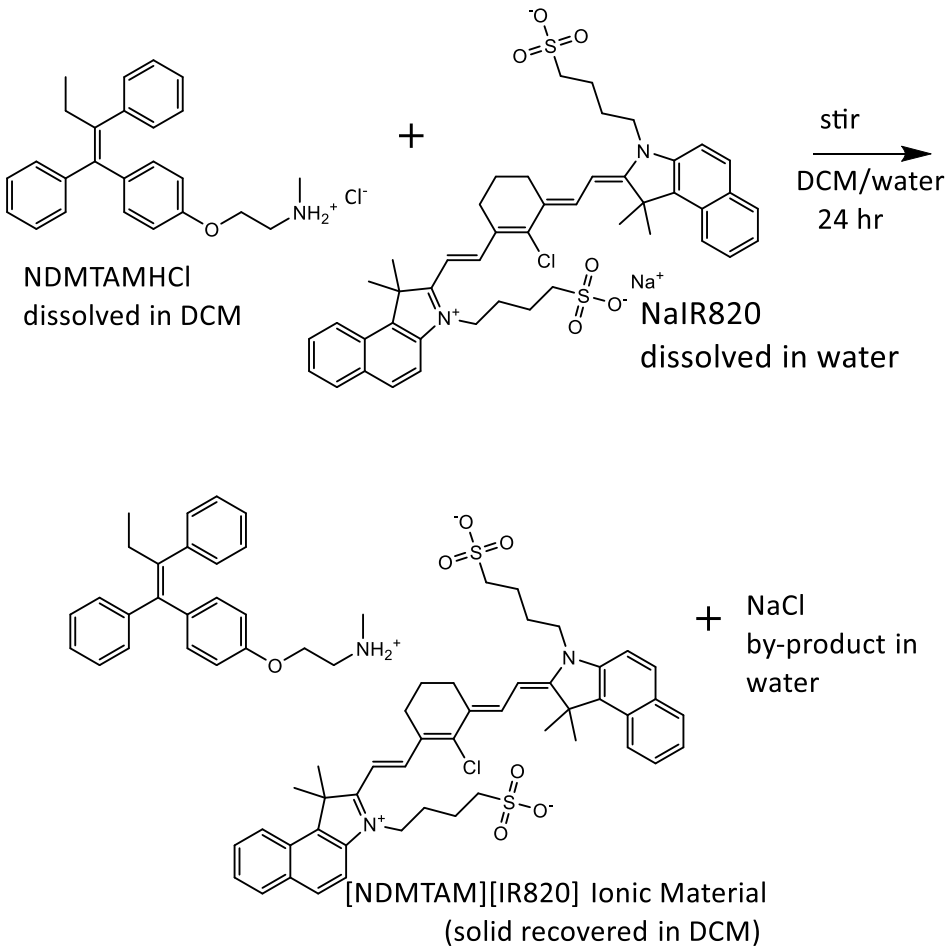

Figure S1: Synthesis scheme for [NDMTAM][IR820] Ionic material.

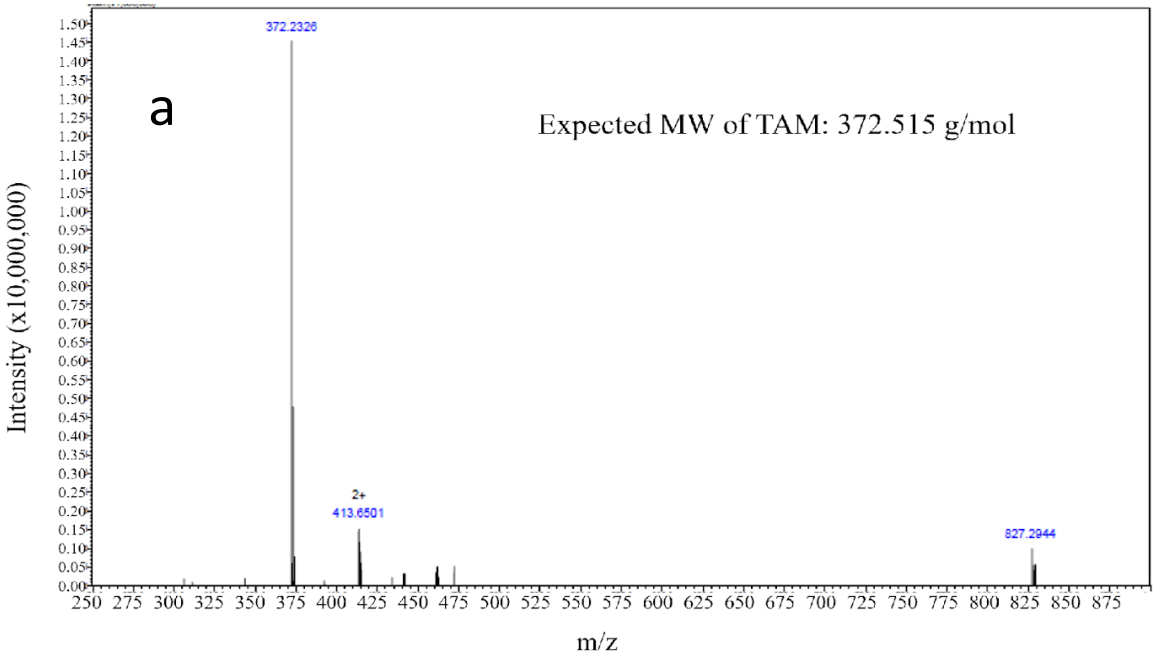

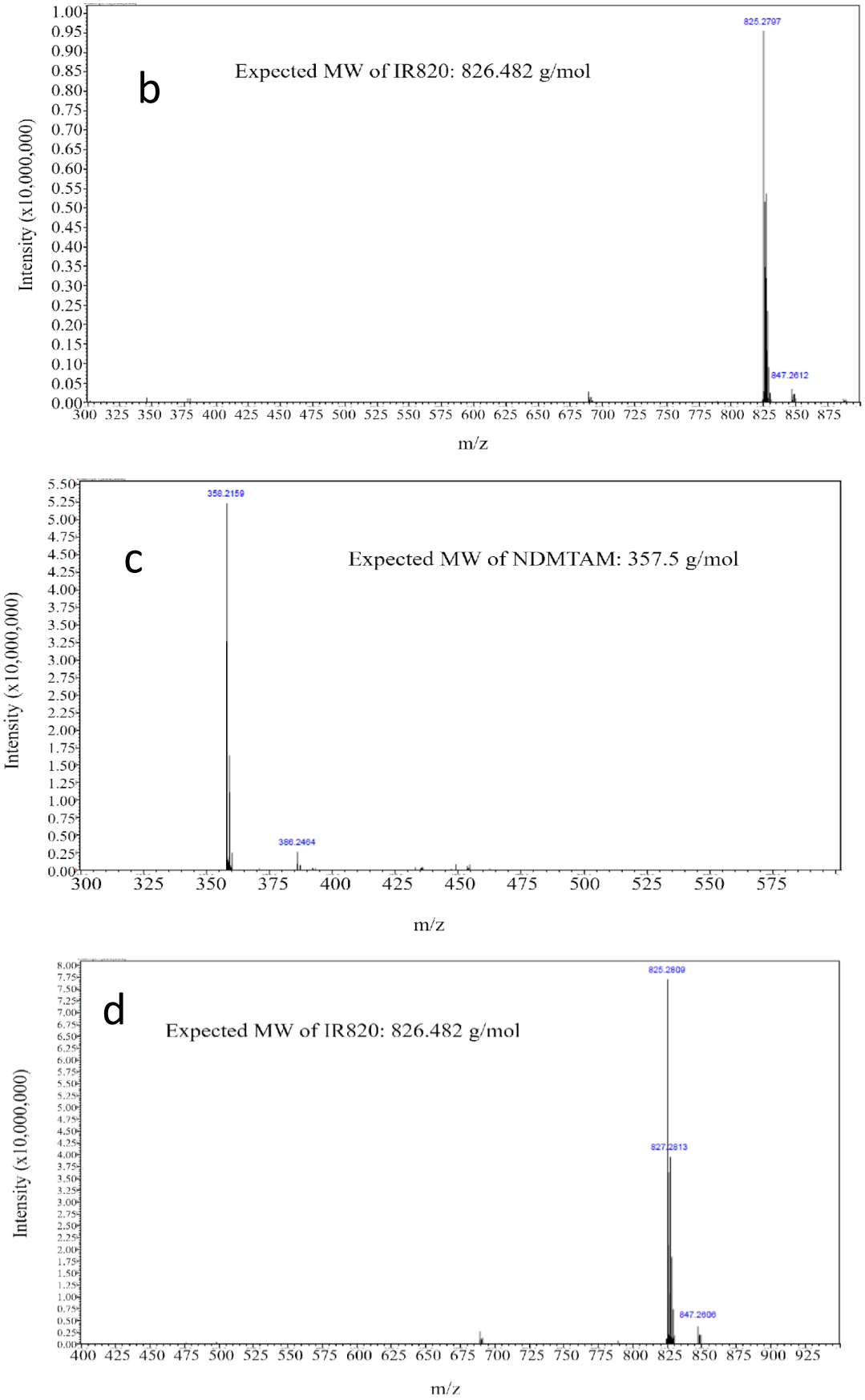

Figure S2: ESI-MS for [TAM][IR820] in the a) positive ion mode b) negative ion mode c) ESI-MS for [NDMTAM][IR820] in the positive ion mode and d) in negative ion mode.

a) NMR spectra of Tamoxifen Hydrochloride

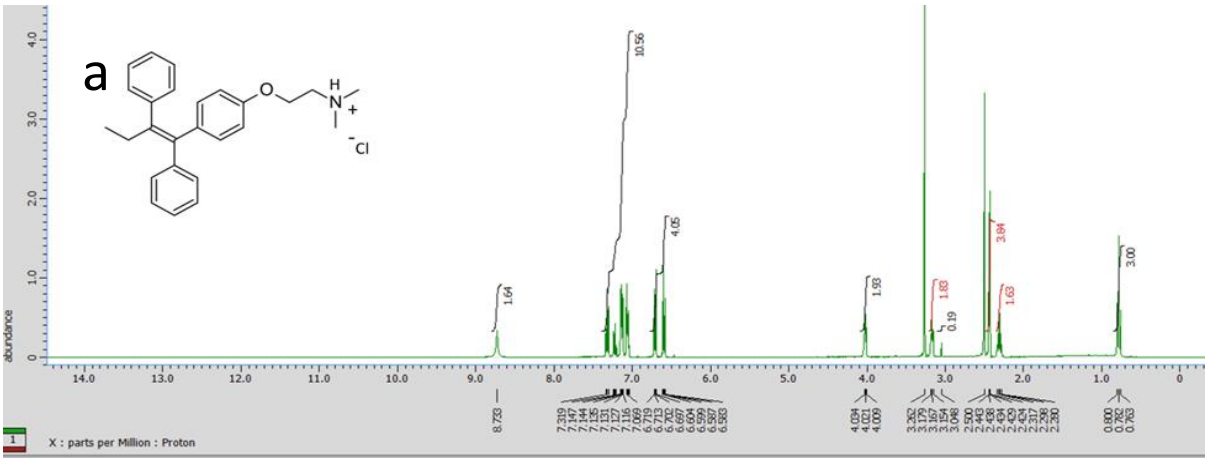

b) NMR spectra of [TAM][IR820]- 1 H NMR (400 MHz, $(CD3)_2SO$): δ 0.8 (m, 3H), 1.9 (m, 19H), 2.4 (d, 2H), 2.8 (d, 9H), 3.4 (d, 1H), 4.1 (t, 2H), 4.3 (t, 3H), 6.4 (m, 2H), 6.7 (m, 4H), 7.1 (m, 10H), 7.5 (m, 2H), 7.7 (m, 2H), 7.9 (m, 2H), 8.1 (m, 4H), 8.3 (m, 4H).

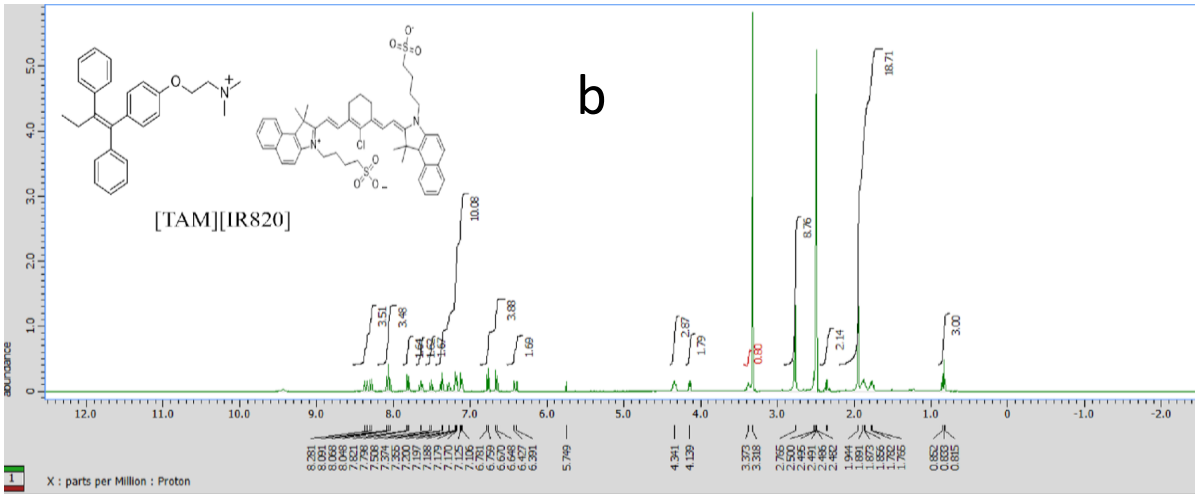

c) NMR spectra of [NDMTAM][IR820]- 1 H NMR (400 MHz, $(CD3)_2SO$): δ 0.8 (d, 3H), 1.9 (m, 14H), 2.4 (m, 2H), 2.6 (d, 3H), 2.8 (m, 3H), 3.2 (d, 1H), 4.0 (d, 2H), 6.4 (m, 1H), 4.7 (m, 4H), 7.3 (m, 12H), 7.5 (m, 4H), 8.1 (m, 3H), 8.4 (m, 5H).

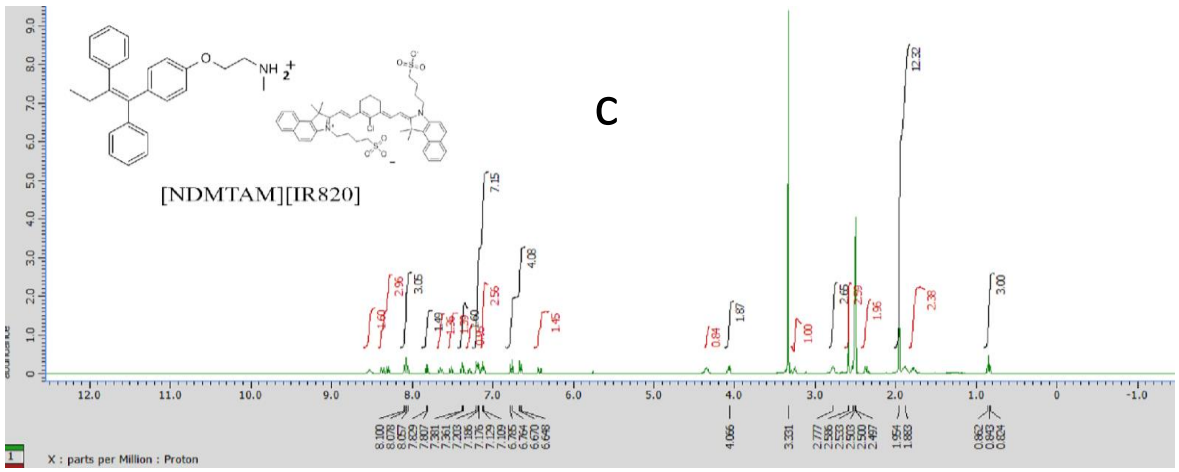

Figure S3: NMR spectrum of a) Tamoxifen hydrochloride b) [TAM][IR820] c) [NDMTAM][IR820].

Table S1: DLS and Zeta potential results for [NDMATM][NIR] and [TAM][NIR] INMs in water.

Sample in water	Size (nm) (48 hrs)	Zeta potential (mV)
[TAM][IR820]	125.3 ± 2.9	-38.2
[NDMTAM][IR820]	116.3 ± 4.6	-28.3

Table S2: Molar absorptivity value of all samples in water (INMs) and ethanol.

Compound/solvent	λ_{max} (nm)	Ɛ ($LMol^{-1}cm^{-1}$) x 10^4
NaIR820_water	688,817	5.98,3.60
[TAM][IR820] _(INMs)	735, 835	7.56, 4.81
[NDMTAM][IR820] _(INMs)	735, 835	6.23, 3.78
NaIR820_ethanol	756, 826	7.25, 23.5
[TAM][IR820] _ethanol	756, 826	8.96, 28.3
[NDMTAM][IR820] _ethanol	756, 826	8.16, 25.6

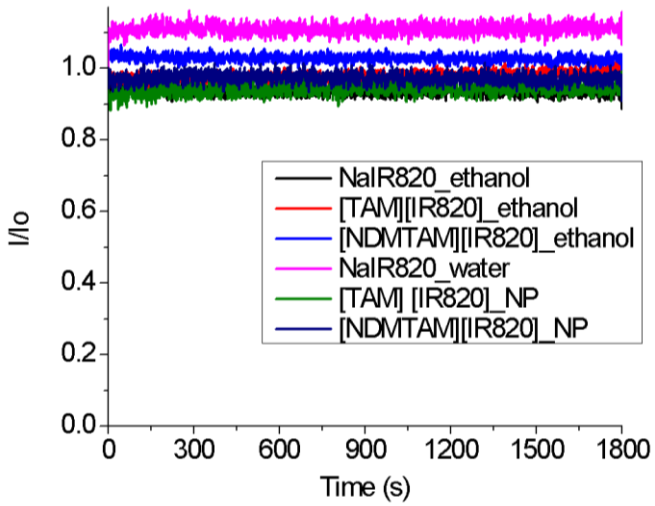

Figure S4: Photostability result for NaIR820 parent compound, derived chemo-PTT IMs and INMs in water and ethanol at 826 nm excitation wavelength.

Photothermal Efficiency

Photothermal heat conversion efficiencies (**η**) of NaIR820 parent compound and its derived INMs were calculated using the following Equation S1-S4

$$\eta = \frac{hs(T_{max} - T_{surr}) - Q_{dis}}{I(1-10^{-A})} \text{ ----------S1}$$

Where h represents the heat transfer coefficient, s is the surface area of the container, and hs is obtained from Equation S4 and Figure 4. T_{max} represents the steady state temperature of the derived INMs and for [TAM][IR820] it was found to be 52.6 ^oC. The environmental temperature (T_{surr}) was 24.1 ^oC. The change in temperature (T_{max} -T_{surr}) for [TAM][IR820] was determined to be 28.5 ^oC. I indicate the laser power, which was 1 W for all samples. A represents absorbance of PTA. Q_{dis} is the heat dissipated from lights absorbed by solution and cuvette walls. Q_{dis} for INMs sample was determined from sample control with pure cell media and was found to be 30.5 mW. To determine hs, the following dimensionless parameter, **θ**, is introduced in Equation S2.

$$\theta = \frac{T - T_{surr}}{T_{max} - T_{surr}} \text{ ----------S2}$$

Then, the time constant τs can be deduced from Equation S3.

$$t = -\tau s \ ln\boldsymbol{\theta}\text{--------S3}$$

Then, the time constant $\boldsymbol{\tau}_s$ of the [TAM][IR820] sample was determined to be 438.9s. By inserting this value into equation S4, hs can be calculated.

$$hs = \frac{m_D c}{\tau_s} \ldots\ldots\ldots S4$$

Where m_D is the mass of solution (1.0 g) and C is the specific heat (4.2 J/g ^oC). hs for [TAM][IR820] was determined to be 9.56 mW/ ^oC. After substituting all parameters into Equation S4, **η** was determined to be 16.96 %.

Reactive oxygen specie generation

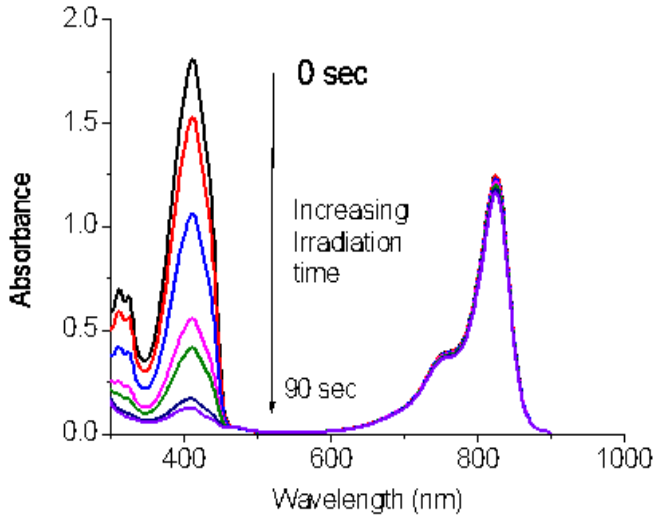

Figure S5: Photodegradation of DPBF upon increasing irradiation time in the presence of [TAM][IR820] in ethanol.

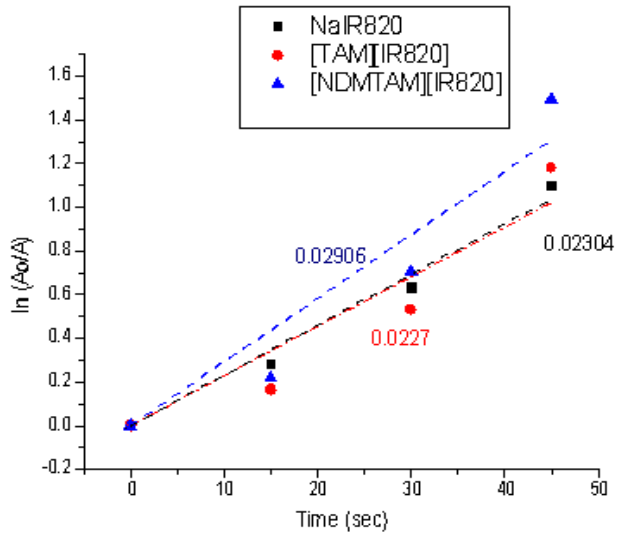

Figure S6: Reactive oxygen quantum yield results in ethanol for NaIR820 parent compound, [TAM][IR820] and [NDMTAM][IR820] IMs.

Table S3: ROS quantum yield for parent NaIR820 dye and its derivatives in ethanol. Concentration of 10 µM of all TAM derivatives and NIR parent dyes with 200 µM DPBF.

Drugs	ROS quantum yield (%)
NaIR820	7.7
[TAM][IR820]	7.8
[NDMTAM][IR820]	10.2

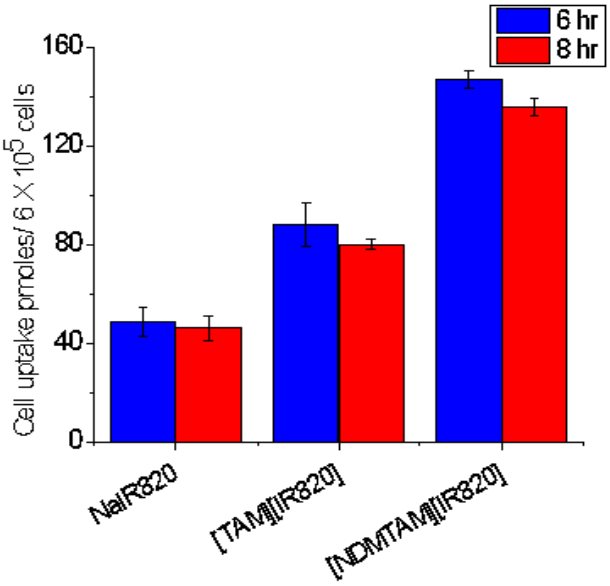

Figure S7: Cellular uptake of INMs compared to free dye after 6 and 8 hr incubation of 50 nmol drug with MCF-7 cancer cells. Data are presented as mean S.D. (n = 3). (*p < 0.05, **p < 0.01, ***p < 0.005).

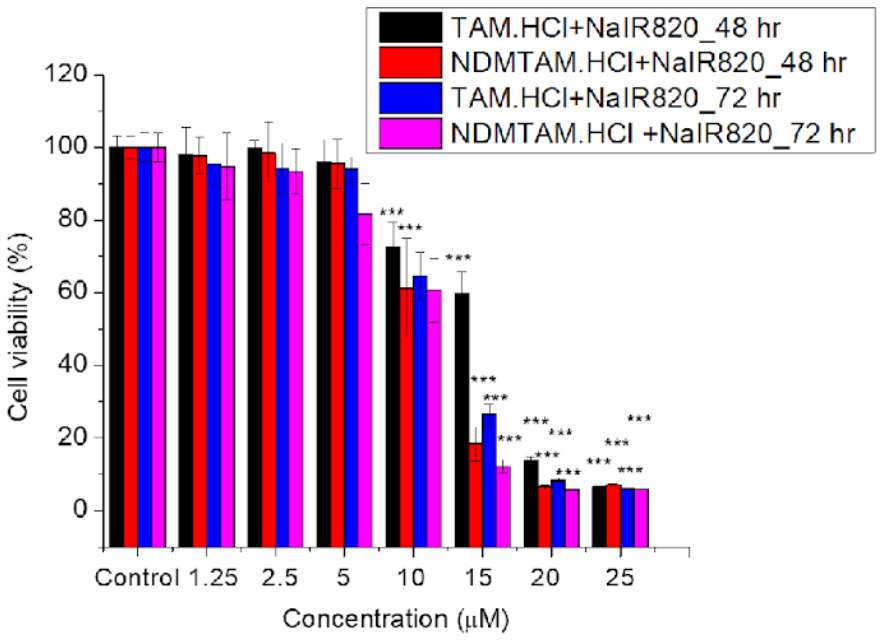

Figure S8: Dark cytotoxicity results for treatment involving 1:1 mixture of chemo and PTT agents in MCF-7 cells at increasing concentrations for 48 hr and 72 hr drug incubation. p values are determined using two-tailed student's t-test and are reported as *p< 0.05, **p< 0. 01, ***p< 0.005.

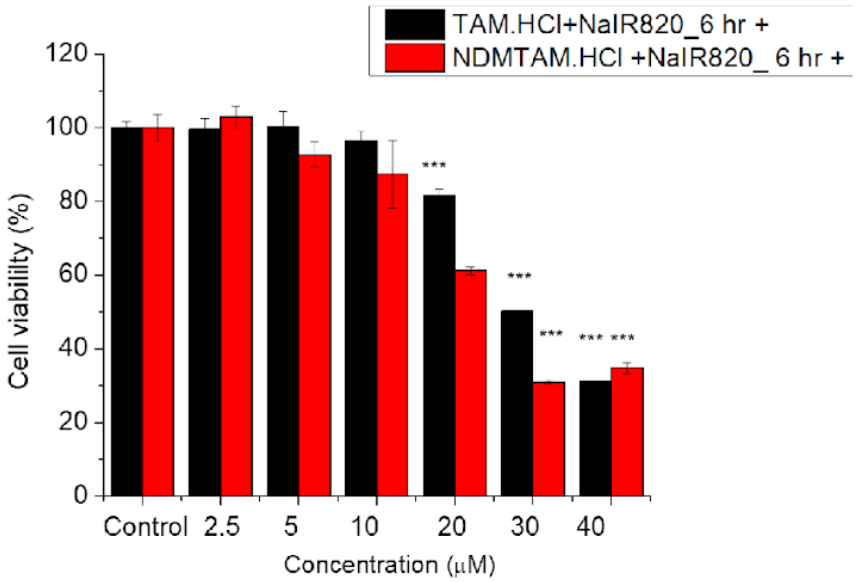

Figure S9: Photo cytotoxicity of treatment involving 1:1 mixture of chemo and PTT drugs in MCF-7 cancer cells incubated for 6 hr followed by 5 min irradiation with 808 nm laser (1 Wcm^{-2}). p values are determined using two-tailed student's t-test and are reported as *p< 0.05, **p< 0.01, ***p< 0.005.